Chapter 3

Scoping and Calibration Experiments

The experimental set-up described in the previous chapter was subjected to various test conditions before conducting actual experiments. Testing of the set-up was carried out to determine the variation of temperature at different locations in the set-up by varying the air flow rate of the air compressor and heating rate of the furnace. Moreover, for accurate sampling of the aerosol generated, it was ensured that isokinetic sampling conditions were maintained during experiments. To meet this objective, an isokinetic probe was designed. The hot exhaust gases had to be cooled before being supplied to the spectrometers for characterization. This required a longer travelling distance through a heat exchanger. In the presence of thermal as well as other gradients in the set-up, various types of losses due to diffusion, gravitational, thermophoresis, and condensation were ascertained.

This chapter is divided into four sections. The variation of temperature of air with different air flow rate and heating conditions is presented in the first section. The results of isokinetic and anisokinetic sampling are provided in the second section. The third section focusses on the transport losses due to diffusion, gravitational and thermophoresis. The last section highlights size distortion in aerosols measurement due to condensation of water vapor on the generated particles.

3.1 Characterization of air temperature

In the present work, graphite samples were placed in the center of an alumina tube which was heated by an array of silicon carbide heating rods. Clean air at different flow rates was passed through the tube. A schematic diagram of the thermocouples arrangement is shown in Figure 3.1. The temperature within the tube at a location close

to the graphite sample was measured by inserting a Platinum-Rhodium (R-type) thermocouple axially into the tube. This temperature is named as the 'inside tube temperature'. Another R-type thermocouple touched the outside of the alumina tube close to the silicon carbide rods. The temperature recorded by this thermocouple is called the 'outside tube temperature' or the 'furnace temperature'. Since alumina is a poor thermal conductor of heat, a significant temperature difference in these two temperatures was expected. The heating profile of furnace is shown in Figure 3.2 where the temperatures measured by both the thermocouples at different air flow rates have been shown. It was found that in the absence of air flow, there was a temperature difference of about 60 °C between the furnace temperature and the inside tube temperature. Most of the heat received by the inner thermocouple is by radiation from the heated walls of the alumina tube, surrounding it. As the air flow was initiated, the difference between the furnace temperature and inside tube temperature increased. As can be seen from Figure 3.2, at a furnace temperature of about 1075 °C, achieved after 400 minutes of heating, the inside tube temperature at a flow rate of 10 $Lmin^{-1}$ was 830 °C, a difference of 245 °C. The thermocouple tip gains heat by radiation from the tube walls and loses heat by convection to the flowing air. When air flow is initiated, the thermocouple comes in contact with cool air, which decreases the tip temperature. An energy balance between these two modes of heat transfer determines the temperature recorded by the thermocouple. An increase in air flow rate results in a higher heat transfer coefficient between the tip and the air, resulting in enhanced convective heat loss and consequently, a reduced inner tube temperature. It was noted that the temperature measured by the inner thermocouple is not the temperature of the air at that location. The inner thermocouple temperature reading takes into account the radiation falling on its stationary tip.

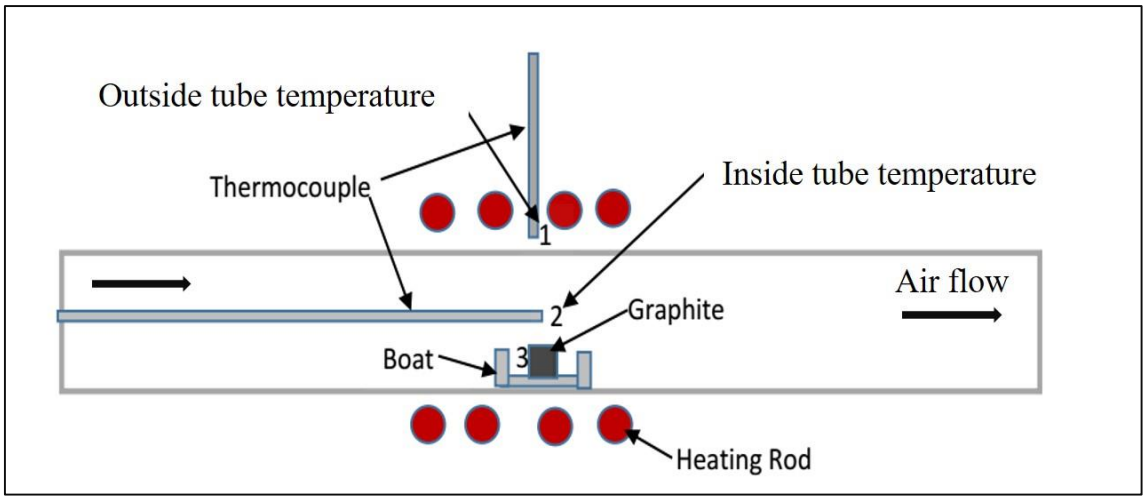

Figure 3.1: Temperature measurement in experiment

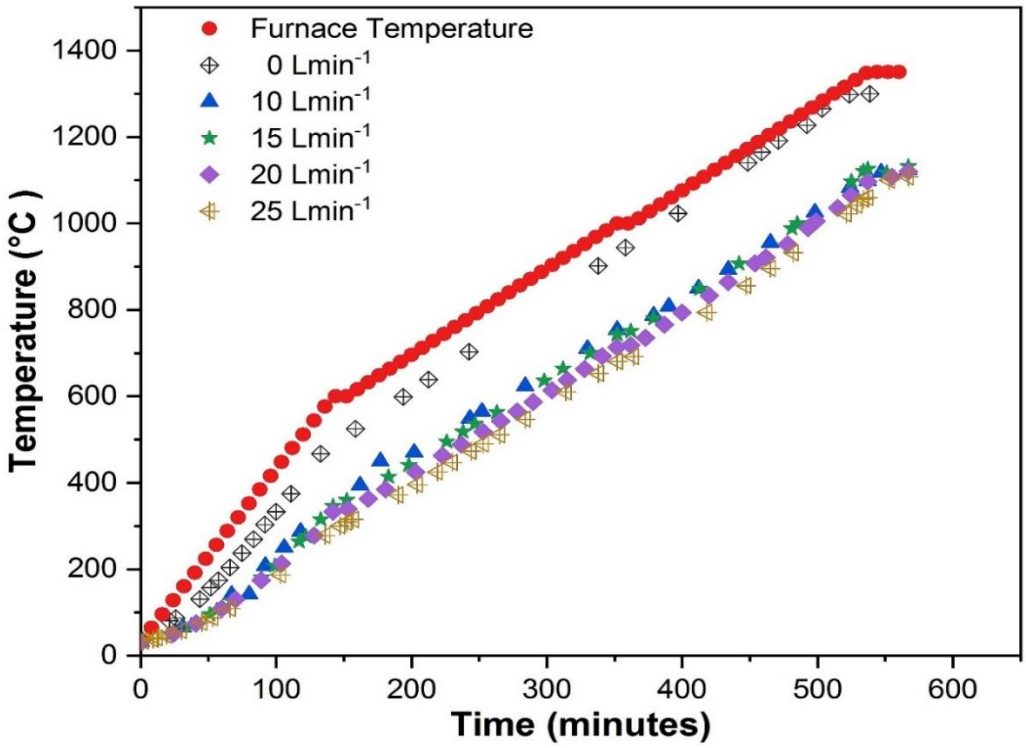

Figure 3.2: Temperature recorded at different flow rates

The hot aerosol, after passing through the alumina tube, flows through the borosilicate tube. It is sampled by passing through an isokinetic probe, placed along the borosilicate tube axis, facing the flow. Since the aerosol passing through the probe is supplied to the spectrometers, it is essential to know its temperature. The maximum aerosol temperature at inlet that the spectrometers can safely handle is 40 °C. The hot

aerosol was cooled by passing it through a heat exchanger before being supplied to the spectrometers. The temperature measured at the port was used for designing heat exchanger.

The borosilicate tube was placed in an environment which was maintained at 20 °C and unlike the alumina tube, there was no intense radiative heating in the borosilicate tube. A fan placed outside the borosilicate tube was used to impart forced convection cooling to the borosilicate tube. Arrangements were made in the set-up for sampling at four ports marked 1, 2, 3, and 4 in Figure 3.3. The air temperature at these sampling ports at a furnace temperature of 1350 °C and air flow rates of 10 - 25 $Lmin^{-1}$ is presented in Figure 3.4. The thermocouple was placed at a location shown in Figure 2.9 (Chapter 2). It is seen that at a given port, the aerosol temperature increases with an increase in air flow rate. For example, at a flow rate of 10 $Lmin^{-1}$, the aerosol temperature at port 1 was about 215 °C, while at 25 $Lmin^{-1}$, it reached 280 °C. The air is heated inside the alumina tube and gets cooled when it flows through the borosilicate tube. It is proposed that at a lower flow rate, the velocity of air is less, leading to its higher residence time in both the tubes. It is expected that at the exit of the alumina tube, the air temperature at a flow rate of 10 $Lmin^{-1}$ would be more than that of air at 25 $Lmin^{-1}$ because the air at 10 $Lmin^{-1}$ resides for a longer time in the heating zone. However, when air at this lower flow rate (and higher temperature) enters the borosilicate tube, it is cooled more as it flows because a larger residence time in the borosilicate tube provides more cooling and its temperature falls more than that of air that flows at higher flow rate (lesser residence time). This explains the observed temperature at different ports as a function of air flow rate.

At a given flow rate, say 10 $Lmin^{-1}$, the aerosol temperature at port 1 was highest and dropped in the direction of flow towards port 4. The reason for this behaviour is that

more time is spent by the aerosol to reach the downstream direction during which it loses more heat, leading to a decrease in temperature.

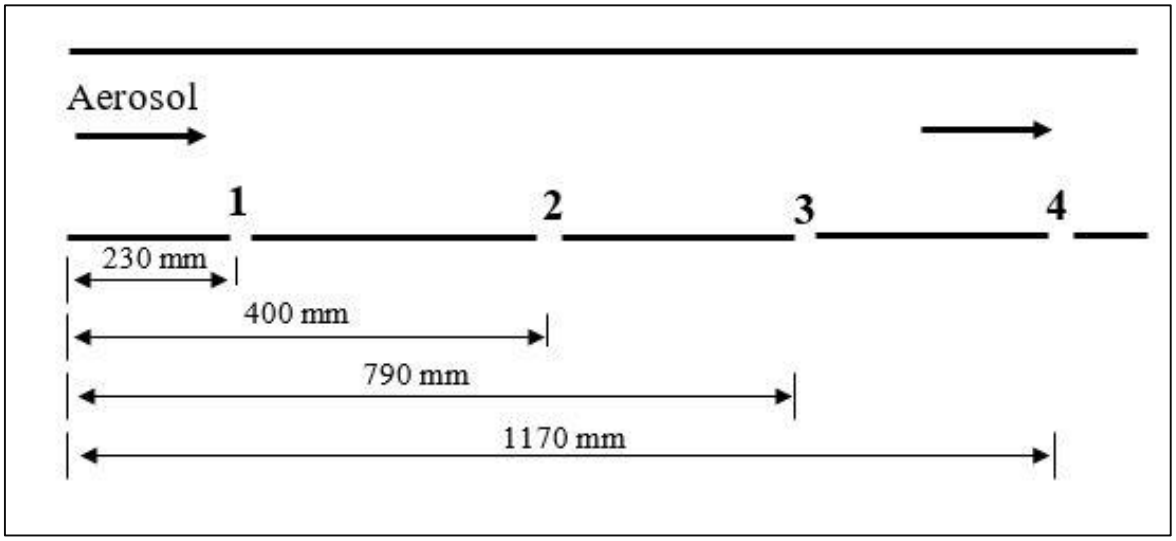

Figure 3.3: Sampling ports in borosilicate tube

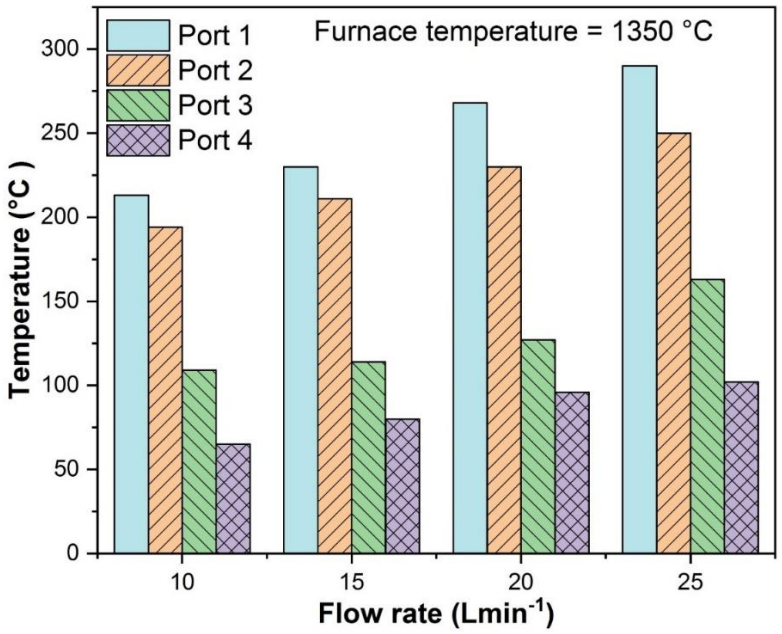

Figure 3.4: Temperature variation at the ports at different flow rate with a constant furnace temperature

3.2 Sampling of aerosol

An essential element in the study of aerosol is the ability to collect a representative sample. The collected sample must accurately reflect the airborne particles in both

concentration and size distribution. A sample of the aerosol is extracted from its environment into an inlet for transport to the measuring instrument. The direction and velocity of the gas from which the sample is taken, the rate of flow of the sample, the orientation of the aerosol sampling probe, the size of the inlet and the geometry and the size of the particles are significant variables in the sampling (Fuchs, 1975). In addition, inertia of particles plays a vital role in aerosol sampling (Von Der Weiden et al., 2009). The inertial behaviour of particles is characterized by a dimensionless number called Stokes number ($Stk.$). The Stokes number is defined as ratio of a characteristic time of particle to a characteristic time of flow (Arouca et al., 2010).

$$Stk. = \frac{\tau U_0}{d_{pr}} = \frac{\tau Q}{A d_{pr}} \tag{3.1}$$

where τ is the relaxation time for a particle to adjust to a change in velocity of the surrounding fluid. U_0 is the average velocity in the tube, and d_{pr} is the diameter of the probe (William C. Hinds, 1999).

$$\tau = \frac{\rho_p d_p^2}{18\eta} \tag{3.2}$$

The viscosity of fluids is calculated by Sutherland equation at mean temperature of air in the tube (William C. Hinds, 1999).

$$\eta = \frac{1.458 \times 10^{-6} T^{1.5}}{T + 110.4} \tag{3.3}$$

Parameters used for calculation: mean temperature of air at the port 1 when flow rates of 10, 15, 20 and 25 $Lmin^{-1}$ is 250 °C, density of particle (ρ_p) is 1820 kg/m^3.

A low value of Stk. (< 0.01) implies that a particle immediately responds to a change in velocity of the surrounding fluid and attains the latter's velocity while a higher value of Stk. means that a particle takes a large time to adjust to a change in the velocity of the surrounding fluid. The Stokes number is a vital parameter in determining the type of

sampling conditions that prevail while characterizing aerosol for their size and size distribution. The importance of Stokes number is described in the following paragraphs.

Figure 3.5 is a schematic representation of a sampling probe placed in an aerosol stream. When airborne particles are sampled in a furnace tube, chimney, internal tubes, ventilation ducts etc., three different flow conditions may arise. These are (a) fluid velocity inside the probe (U) equals to the fluid velocity inside the tube (U_0), i.e. $U = U_0$ (b) $U > U_0$ (c) $U < U_0$. During the first condition, shown in Figure 3.5(a), the fluid streamlines in the tube are not disturbed by the introduction of the probe in its path and the aerosol concentration in the probe is equal to the concentration in the tube (William C. Hinds, 1999). This is called an isokinetic sampling condition. If the sampling is isokinetic, there is no particle loss at the inlet of the probe, regardless of particle size or inertia. When $U > U_0$, fluid streamlines in the tube get diverted towards the probe. Particles with larger inertia are unable to change their trajectory and continue to move straight and fail to enter the probe while smaller particles with lesser inertia follow the converging streamlines and are able to enter the probe. Under such a condition, the measured concentration underestimates the true concentration, and too few large-sized particles are measured. This condition is called a super-isokinetic condition (Figure 3.5(b)). When $U < U_0$, the fluid streamline diverges at the probe inlet, and some large particles that are unable to flow with the streamlines, enter into the probe, resulting in an overestimated concentration of larger particles. This condition is called sub-isokinetic sampling (Figure 3.5(c)). The super and sub-isokinetic sampling is together also called non-isokinetic or anisokinetic sampling. Hence, we can conclude that isokinetic sampling is ensured when (a) Stk. << 0.01 and (b) $\frac{U_0}{U} = 1$.

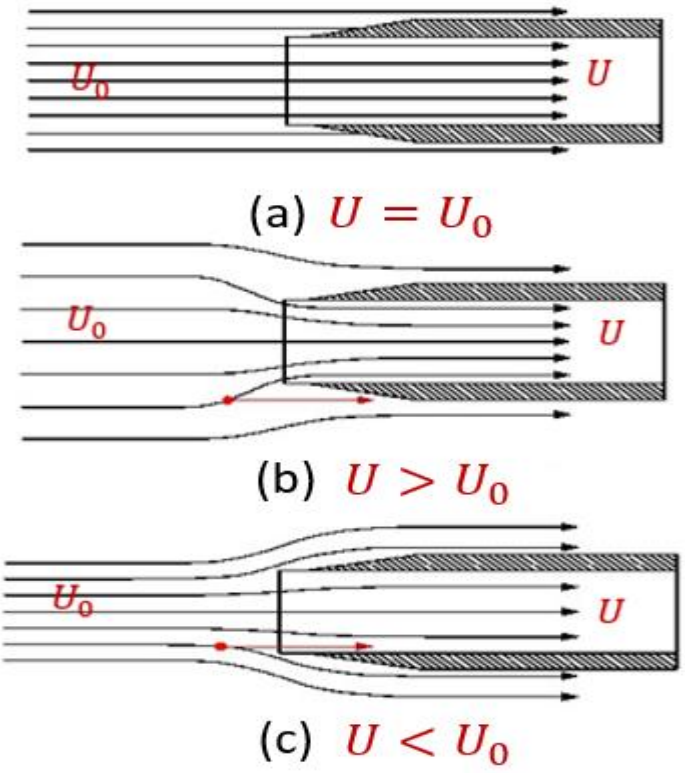

Figure 3.5: Schematic diagram of the sampling at (a) isokinetic (b) super-isokinetic (c) sub-isokinetic conditions

Unless the initial particle size distribution is known or can be estimated, there is no way to determine the actual concentration if sampling is not done isokinetically. The conditions that must be fulfilled to achieve isokinetic sampling are summarized below:

1. Stokes number << 0.01
2. The axis of the sampling probe should be aligned parallel to the gas streamline.
3. The free stream velocity in the tube should equal the velocity of the gas entering the probe.
4. Particles should be captured by the probe in such a way that they do not deviate from their original path.

The issue of misalignment of probe, when the probe is not positioned axially with the fluid stream was studied by Durham (Durham and Lundgren, 1980). They gave an

empirical relation for misalignment of a probe when $0° \leq \Theta \leq 90°$ (Θ is angle between the flow direction and sampling probe) and 0.01 < Stk. < 6.

$$\frac{C}{C_0} = 1 + (\cos\Theta - 1)\left(1 - \frac{1}{1 + 0.55(Stk') \exp(0.25Stk')}\right) \tag{3.4}$$

where

$$Stk.' = Stk.exp.(0.022\,\Theta) \tag{3.5}$$

Belyave and Levin gave an empirical equation for the case when the probe is aligned properly but the sampling is anisokinetic (0.01 < Stk. < 6) (Belyaev and Levin, 1974).

$$\frac{C}{C_0} = 1 + \left(\frac{U_0}{U} - 1\right)\left(1 - \frac{1}{1 + \left(2 + 0.62\frac{U}{U_0}\right)Stk}\right) \tag{3.6}$$

Brockman provided an empirical relationship when considering both velocity ratio and probe misalignment (Stk. > 6) (Baron, 2011).

$$\frac{C}{C_0} = \frac{U}{U_0}\cos\Theta \tag{3.7}$$

Research on anisokinetic sampling shows that particle concentration in the sampling probe changes with velocity ratio ($\frac{U_0}{U}$) and Stokes number (Stk.).When Stk. << 0.01 and $0.2 < \frac{U_0}{U} < 5.0$, aerosol particles approximately follow the gas streamlines, the anisokinetic sampling loss is negligible and isokinetic sampling condition is approximately (not exactly) ensured, i.e. $\frac{C}{C_0} \approx 1$ (William C. Hinds, 1999).

An estimate of the maximum Stokes number in this work was found out to determine the sampling condition (isokinetic or anisokinetic). It can be inferred from eq. 3.1 and 3.2, that for identical flow velocity in tube and probe diameter, larger the particle diameter, larger the Stokes number and vice-versa. In the present work, the maximum possible diameter of the generated aerosol was used to calculate the upper limit of the

Stokes number. During experiments, the maximum diameter of the generated aerosol was found to be about 400 nm. Hence, the Stokes number for a 400 nm particle (and a relaxation time of 6.89×10^{-7} s) at different flow rates and probe diameters was calculated and is presented in Figure 3.6. It can be seen that the Stokes number is less than 0.01 for probe diameters lying in the range of practical interest (5 - 40 mm) and flow rates (10 - 25 $Lmin^{-1}$) used in the experiments. The upper range of probe diameter of practical interest (40 mm) was determined by consideration of the inner diameter of the borosilicate tube (70 mm). Any larger size of the probe would be very difficult to position inside the tube. A probe diameter of less than 5 mm diameter would have created difficulty in cleaning. Hence the choice of the probe diameter range was taken as 5 - 40 mm.

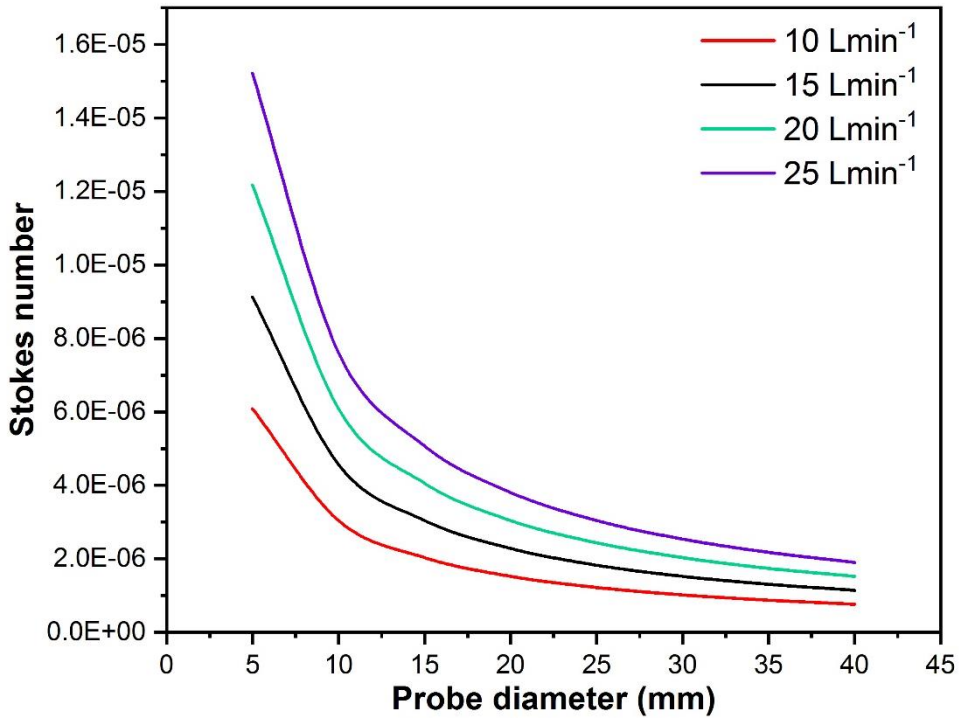

Figure 3.6: Variation of Stokes number with the probe diameter at different flow rate

Once it was proved that one of the conditions for isokinetic sampling (Stk. << 0.01) was satisfied, we sought to find out the probe diameter for the case $0.2 < \frac{U_0}{U} < 5.0$. A probe diameter satisfying this inequality would then guarantee near isokinetic sampling.

The diameter of the probe for isokinetic sampling is determined from the expression (Ram et al., 1995):

$$\frac{U_0}{U} = \frac{Q}{q}\left(\frac{d_{pr}}{D_T}\right)^2 \tag{3.8}$$

The probe diameter for isokinetic condition at a particular flow rate Q is obtained by putting the LHS of eq. 3.8 equal to 1.0 ($\frac{U_0}{U} = 1$), tube diameter (D_T) = 70 mm and q = 1.8 $Lmin^{-1}$. A value of 1.8 $Lmin^{-1}$ has been used here because this is the combined flow rate of the Nanoscan and OPS. It is evident that the isokinetic probe diameter will depend on Q. Hence, one isokinetic probe for a tube flow rate of 10 $Lmin^{-1}$ was fabricated and used for all flow rates. The level of error introduced by the resulting non isokinetic sampling at flow rates of 15, 20 and 25 $Lmin^{-1}$ was estimated.

Since the other condition for near isokinetic sampling is $0.2 < \frac{U_0}{U} < 5$, the probe diameter for the lower and upper limiting values of $\frac{U_0}{U}$ and different flow rates was calculated using eq. 3.8 and the results are presented in Table 3.1. It is seen that if the probe diameter lies in the range 13.3 - 42 mm, near isokinetic conditions are obtained for a flow rate in the range 10 - 25 $Lmin^{-1}$.

Table 3.1: Probe diameter range at different flow rates

Flow rate in tube ($Lmin^{-1}$)	**When $0.2 < \frac{U_0}{U} < 5$ probe diameter range (mm)**
10	13.3 - 66.4
15	10.8 - 54.2
20	9.4 - 47.0
25	8.4 - 42.0

The isokinetic probe diameter for 10 $Lmin^{-1}$ was calculated to be 29.7 mm. This diameter lies within the range of 13.3 – 42.0 mm.

The effects of anisokinetic sampling can be verified by (i) using a probe diameter of 29.7 mm at flow rates of 15, 20 and 25 $Lmin^{-1}$ or (ii) using probe diameters different from 29.7 mm (but within 13.3 - 66.4 mm range) at 10 $Lmin^{-1}$. The first choice was rejected because the aerosol generation depends strongly on the flow conditions. Varying flow rate would produce different particle size distribution, thereby making a comparison impossible and thus rendering the whole exercise futile. The other option was adopted and two probes of diameter 15 and 33 mm respectively were tested at 10 $Lmin^{-1}$. The first probe diameter resulted in a super-isokinetic sampling while the latter produced a sub-isokinetic sampling. Together, they resulted in anisokinetic sampling conditions.

Graphite powder weighing 14 gm was burnt and the aerosol produced was used to compare isokinetic and anisokinetic sampling at a flow rate of 10 $Lmin^{-1}$. The heating rate shown in Figure 3.2 was used for these experiments. The experimental conditions for isokinetic and anisokinetic sampling are mentioned in Table 3.2. A set of ten experiments were conducted for the isokinetic condition and five each for the super and sub isokinetic sampling. The instrument records reading for 13 channels (bins) after a duration of every one minute. The time-averaged number concentration for a 9 hours sampling duration for each channel size was calculated. The mean of these ten values is presented in Figure 3.7. The difference in the mean number concentration values for isokinetic and anisokinetic sampling was 10% for the 10.0 - 15.4 nm range and 4.6% for the 86.6 - 115.5 nm range. The mean of this difference for the 13 channels was found to be 6%. From the above results, it can be inferred that this error be neglected. Hence a probe diameter of 29.7 mm was used for the different flow rates.

Table 3.2: Experimental conditions for isokinetic and anisokinetic sampling

Experimental condition	d_{pr} (mm)	Q ($Lmin^{-1}$)	U_0 (m/s)	U (m/s)	U_0/U
Isokinetic sampling [a]	29.7	10	0.04	0.04	1
Anisokinetic sampling (d_{pr})[b]	15	10	0.04	0.38	0.2
	33	10	0.04	0.03	1.3

a 10 trial runs
b 5 trial runs

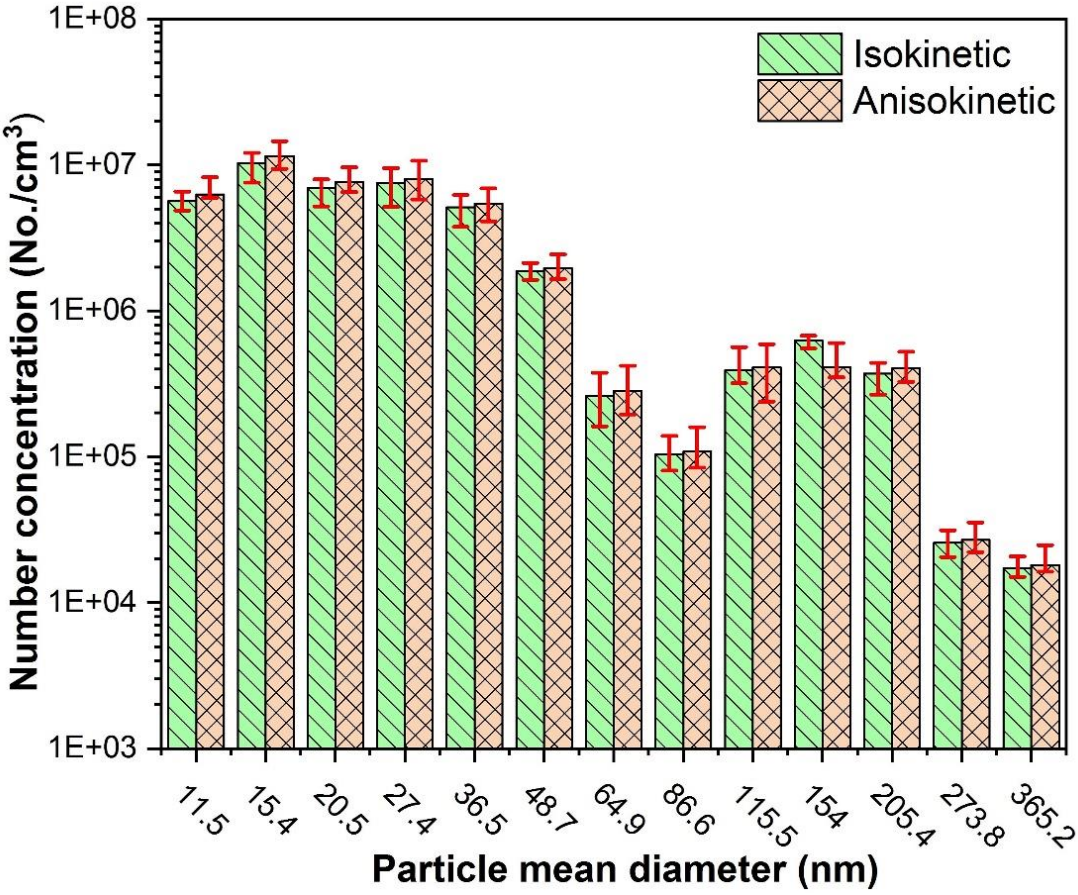

Figure 3.7: Comparison of isokinetic and anisokinetic sampling

3.3 Transport of aerosol

Most aerosol measurements require an inlet system to transport aerosol from a selected sampling location to a suitable measuring device through some length of tubing. These tubes may contain contractions, bends, slopes and other flow elements (Von Der

Weiden et al., 2009). During transit, particles get deposited at various obstructions before they can reach the measuring instrument, resulting in a loss in the number of particles generated and those that reach the measuring instrument. Particle loss may also occur in the tubes due to physical phenomena of electrostatic attraction, impaction, gravitational settlement, diffusion, thermophoresis etc. (Baron, 2011). These losses are collectively termed as transport losses. The distinct behavior of particles depends on their size range, their flow regime (laminar or turbulent) and the physical laws governing their motion. For a fluid in laminar flow, Brownian, gravity, thermophoretic and lifting forces primarily affect the deposition of the particles while for a turbulent flow, additional forces due to turbulent diffusion and turbulent collision also become operational. Additionally, small-sized particle motion is governed by Brownian motion, while large-sized particles are influenced by inertia and gravitational forces. Depending on the aerodynamic size of the particle, a variety of particle loss mechanisms could be effective in any particle measurement (William C. Hinds, 1999).

During measurement of aerosol, the loss of particles alters its characteristics. To reduce loss, the transport lines must be made of a conductive material in order to decrease the electrostatic loss. Furthermore, contractions, bends, steep slope and large length of these lines must be minimized. In the present research, aerosol measurements were carried out using aerosol spectrometers, which were attached to the sampling probe by means of a conductive, circular connecting tube of uniform diameter with minimum bends and slope to minimize transport losses. The Reynolds number of flow was calculated and its values have been shown in Table 3.3. It can be seen that for all test conditions, Reynolds number was less than 2000. Hence the flow was laminar and the particle deposition by turbulent diffusion and turbulent collision was expected to be

negligible. Brownian motion, gravity and thermophoretic force were expected to the major factors affecting the transport loss.

Table 3.3: Reynolds number at different flow rates

Volume flow rate ($Lmin^{-1}$)	**Velocity in duct (m/s)**	**Reynolds number ($Re = \frac{\rho_p U_0 D_T}{\eta}$)**
10	0.04	65.0
15	0.06	97.5
20	0.08	130.1
25	0.11	162.6

Transportation losses can be either determined experimentally or estimated using empirical correlations. In this work, for the experimental determination of transport losses, sampling from two locations, one close to the burning sample and other farther away would have to be done. This would require a pair of measuring instruments like Nanoscan, OPS, diluter etc. Since these many equipment were not available, experimental determination of transport losses was not possible and the transport losses were estimated using empirical correlations taken from standard textbooks of Aerosol Technology and Research Paper (Baron, 2011; William C. Hinds, 1999). The estimation of these losses gives an idea of the uncertainty of the measured results.

3.3.1 Diffusion loss

Gas molecules, undergoing Brownian motion, rebound when they collide with a surface and transfer momentum with the wall. This transfer of momentum is the mechanism by which gas pressure is transferred to the surface of the tube. Unlike gas molecules, aerosol particles adhere to the tube surface when they collide. The surface of the tube acts as a sink for these diffusing aerosol particles and the concentration at the

wall is taken to be zero for mathematical analysis. A concentration gradient is established in the region near the tube surface. Following the Fick's law of diffusion, the concentration gradient causes a continuous diffusion of aerosol particles towards the surface, resulting in a gradual decrease of concentration in the tube. This loss is called diffusion loss (Durham and Lundgren, 1980; Lee and Kim, 1999).

The following equations were used to calculate the diffusion loss (%) of the system (William C. Hinds, 1999):

$$\eta_{tube,diffu.} = (1 - P_0) \times 100 \tag{3.9}$$

$$P_0 = 1 - 5.50\mu^{\frac{2}{3}} + 3.77\mu \qquad For\ \mu < 0.009 \tag{3.10}$$

$$P_0 = 0.819\exp(-11.5\mu) + 0.0975\exp(-70.1\mu) \qquad \mu \geq 0.009 \tag{3.11}$$

where, P_0 is deposition efficiency, μ is the dimensionless deposition parameter.

$$\mu = \frac{DL}{Q} \tag{3.12}$$

$$D = kTB \tag{3.13}$$

$$B = \frac{C_c}{3\pi\eta d_p} \tag{3.14}$$

$$C_c = 1 + \frac{1}{pd_p}\left(15.60 + 7.00\exp(-0.059pd_p\right) \tag{3.15}$$

Parameters used for calculation: length of the tube (distance between the center of the aluminum tube and port 1) = 0.55 m, mean temperature of air at the center of tube when flow rates of 10, 15, 20 and 25 $Lmin^{-1}$ = 350 °C, mean temperature of air in tube = 300 °C, P is the atmospheric pressure. In the present study, the maximum value of μ was calculated to be 7.2×10^{-7} Pa.s (Baron, 2011).

Diffusion losses were calculated for different particle sizes with an air flow range of 10 - 25 $Lmin^{-1}$ and the results are shown in Figure 3.8. The system's diffusion losses are

shown to be small with a maximum value of 1.7% for a 10 nm particle at 10 $Lmin^{-1}$ flow rate.

3.3.2 Gravitational loss

The gravitational force is the major parameter responsible for the aerosol deposition in a horizontal pipe. The larger sized particles easily settle down on the bottom surface of the pipe due to gravity, thus causing particle loss. Since the flow is laminar in this research, expression of particle deposition due to gravity in a horizontal tube under laminar flow conditions is given as (Thomas, 1958):

$$Gravitational\ loss\ (\%)\ =\ (1-\eta_{tube,grav})\ \times\ 100 \tag{3.16}$$

$$\eta_{tube,grav} = 1 - \frac{2}{\pi}\left[2\varepsilon\sqrt{1-\varepsilon^{\frac{2}{3}}}\ - \varepsilon^{\frac{1}{3}}\sqrt{1-\varepsilon^{\frac{2}{3}}} + arc\ sin\left(\varepsilon^{\frac{1}{3}}\right)\right] \tag{3.17}$$

where

$$\varepsilon = \frac{3}{4}Z \tag{3.18}$$

where Z is the gravitational parameter which is calculated as

$$Z = \frac{L\,V_{ts}}{U_0 D_T} \tag{3.19}$$

$$V_{ts} = \frac{\rho_p d_p^2 g C_c}{18\eta} \tag{3.20}$$

Parameters used for calculation: length of the tube (L) = 0.55 m, tube inner diameter = 0.07 m.

Using these values, the maximum gravitational loss for all particle diameters less than 365.20 nm was estimated to be less than 0.25%. These results are shown in Figure 3.8.

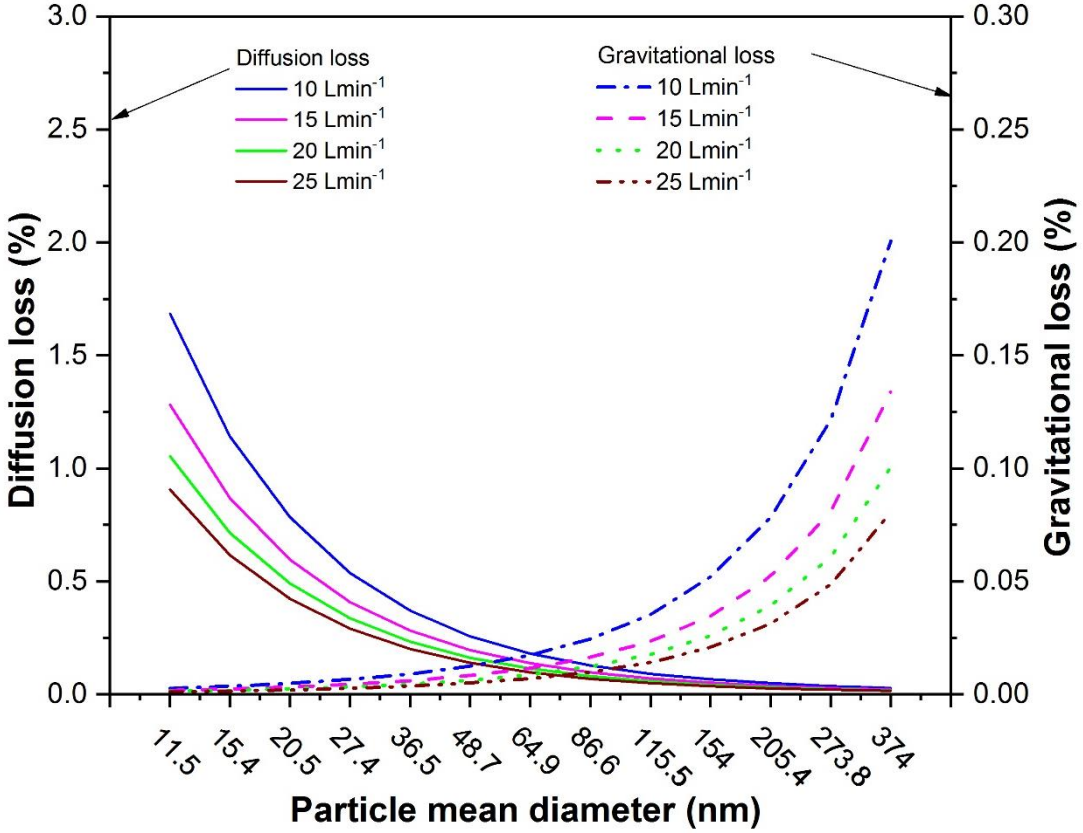

Figure 3.8: Variation of diffusion and gravitational loss with particle mean diameter at different flow rates

3.3.3 Thermophoresis loss

When a temperature gradient is established in a gas, an aerosol particle in that gas experience a force in a direction of decreasing temperature. The movement of the particles that results from this force is called thermophoresis. The thermophoresis force and the aerosol particle motion are always in the direction of decreasing temperature. When a cold surface is close to a warm gas, thermophoresis causes particles in the gas to be deposited on to the surface. This phenomenon leads to a thermophoresis loss.

In the present study, the heated aerosol from the alumina tube comes into contact with the colder wall of the borosilicate tube where thermophoretic losses may occur in the experimental set-up. The thermophoretic deposition efficiency is a function of the

thermophoretic coefficient (k_{th}), Prandtl number (Pr), dimensionless temperature for fully developed laminar flow (Tsai et al., 2004):

$$\eta_{ther.loss}(\%) = 78.3 \left(Pr\ k_{th} \frac{T - T_w}{T_w} \right)^{0.94} \tag{3.21}$$

where k_{th} is defined as in (Talbot et al., 1980):

$$k_{th} = \frac{2C_c C_s}{1 + 3C_m \left(\frac{2\lambda}{d_p}\right)} \times \frac{\frac{k_g}{k_p} + C_t \left(\frac{2\lambda}{d_p}\right)}{1 + 2\frac{k_g}{k_p} + 2C_t \left(\frac{2\lambda}{d_p}\right)} \tag{3.22}$$

where

C_m (momentum exchange coefficient) = 1.14

C_s (thermal slip coefficient) = 1.17

C_t (temperature jump coefficient) = 2.18

k_g(thermal conductivity of gas) = 0.052 W/mk

λ is the molecular mean free path.

All these parameter was taken from the Tablot et. al., 1980.

$$\lambda = \lambda_r \frac{101}{p} \times \frac{T}{293} \times \frac{1 + \frac{110}{293}}{1 + \frac{110}{T}} \tag{3.23}$$

where the wall temperature of the borosilicate tube (T_w) was measured to be 450 K, λ_r = 5.64× 10^{-8} m, the thermal conductivity of the particles (k_p) = 68 W/mK, all values were calculated at an average air temperature (T) of 300 °C and atmospheric pressure.

The maximum thermophoretic loss for a particle diameter of 365.20 nm was found to be about 5.0% (Figure 3.9).

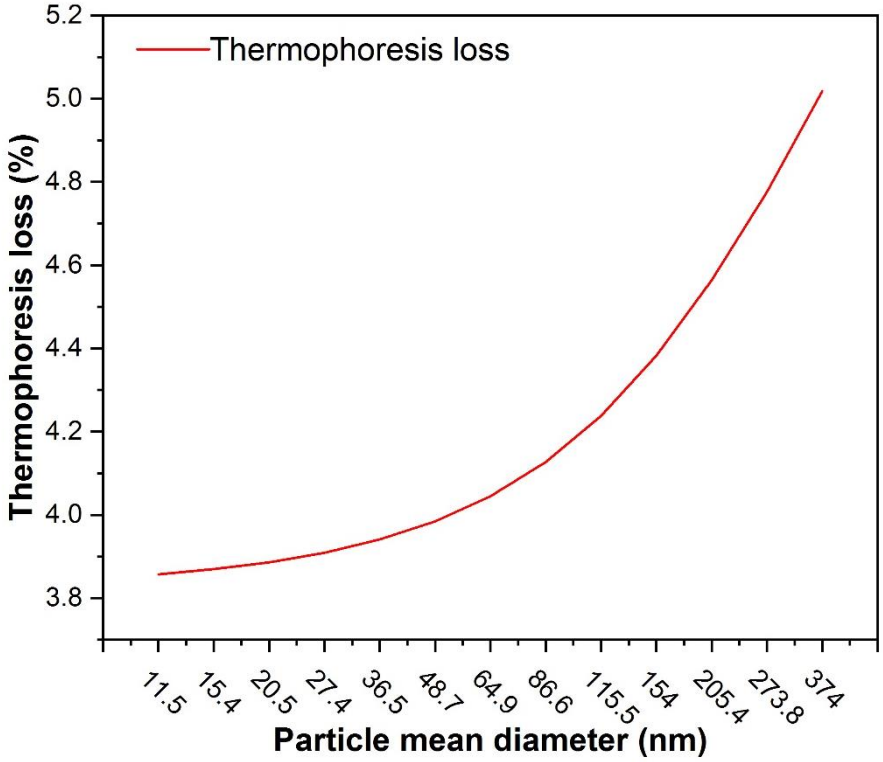

Figure 3.9: Variation of thermophoresis loss with particle mean diameter

The total transport loss is the product of the transport loss for each mechanism (Baron, 2011):

$$\eta_{\text{tube,total loss}} = \eta_{\text{tube,grav}} \times \eta_{\text{ther.loss}} \times \eta_{tube,diffu.} \quad (3.24)$$

From eq. 3.24, it was found that the general losses due to diffusion, thermophoretic and gravitational settlement were less than 5.0%, which can be neglected.

3.4 Condensation of water vapor present in air

Aerosol size is a function of pressure, temperature, relative humidity and concentration of vapor in air. The size of aerosol containing volatile species or condensable vapors may be altered by changing these parameters. Disturbance of the vapor equilibrium due to alteration of the pressure, relative humidity and temperature results in a size distortion of aerosol. Extreme conditions like exceeding 100% relative humidity are encountered occasionally.

The condensation of water vapor occurs whenever the temperature reaches below the dew point. In the present set-up, at the inlet of the alumina tube, the air temperature and relative humidity were measured to be 25 °C and 60% respectively. At these conditions, the humidity of the air was calculated to be 13.86 gm/m^3. In the experimental set-up, the humidity of the air remained constant as no mass of water vapors was added or bleed out of it. At the inlet and outlet of the heat exchanger, temperatures were measured to be 250 °C and 40 °C respectively, and corresponding values of the relative humidity were calculated to be 0.67% and 27.15% respectively. Since the relative humidity is less than 100% in the entire set-up, no condensation would occur and hence no particle size bias would be present due to condensation.

Summary

In this chapter, the variation of temperature at different locations in the set-up was measured. Sampling of graphite aerosol was performed using an isokinetic probe designed for this purpose. Different tests were conducted to study the effect of isokinetic and anisokinetic sampling for aerosol particles in the laminar flow regime in a tube. Isokinetic, sub isokinetic and super isokinetic condition were tested, and the findings show that sampling of nanometric sized aerosol does not depend on flow rates in the tube for the range 10 - 25 Lmin^{-1} and the diameter of sampling nozzle for Stokes number less than 0.01 and $0.2 < \frac{U_0}{U} < 5.0$. It was confirmed that the 29.70 mm diameter sample could be used for distinct air flow rates to measure the number concentration of the particle. Transport losses due to diffusion, thermophoresis and gravitational settlement were calculated to be less than 5%. Calculated and found negligible effects of condensation on particle concentration and size distribution measurement.

References

Arouca, F.O., Feitosa, N.R., Coury, J.R., 2010. Effect of sampling in the evaluation of particle size distribution in nanoaerosols. Powder Technol. 200, 52–59. https://doi.org/10.1016/j.powtec.2010.02.007

Baron, P.A., 2011. Aerosol Measurement Principles, Techniques, and Applications, 3rd ed, A Jhon Willey & Sons. Inc. Publication. Willey, Canada. https://doi.org/10.1016/0021-8502(80)90037-3

Belyaev, S.P., Levin, L.M., 1974. Techniques for collection of representative aerosol samples. J. Aerosol Sci. 5, 325–338. https://doi.org/10.1016/0021-8502(74)90130-X

Durham, M.D., Lundgren, D.A., 1980. Evaluation of aerosol aspiration efficiency as a function of Stokes number, velocity ratio and nozzle angle. J. Aerosol Sci. 11, 179–188. https://doi.org/10.1016/0021-8502(80)90033-6

Fuchs, N.A., 1975. Review Papers Sampling of Aerosol. Atmos. Encironment 9, 697–707.

Lee, K.W., Kim, S.P., 1999. Analytical solutions to diffusional deposition of polydisperse aerosols in parallel plate channels and circular tubes. Aerosol Sci. Technol. 31, 56–65. https://doi.org/10.1080/027868299304354

Ram, M., Cain, S.A., Taulbee, D.B., 1995. Design of a shrouded probe for airborne aerosol sampling in a high velocity airstream. J. Aerosol Sci. 26, 945–962. https://doi.org/10.1016/0021-8502(95)00029-C

Talbot, L., Cheng, R. k, Schefer, R.W., Willis, D.R., 1980. Thermophoresis of particles in a heated boundary layer. J. Fluid Mech. 101, 737–758.

Thomas, J.W., 1958. Gravity settling of particles in a horizontal tube gravity settling of particles in a horizontal tube. J. Air Pollut. Control Assoc. 8, 32–34. https://doi.org/10.1080/00966665.1958.10467825

Tsai, C.J., Lin, J.S., Aggarwal, S.G., Chen, D.R., 2004. Thermophoretic deposition of particles in laminar and turbulent tube flows. Aerosol Sci. Technol. 38, 131–139. https://doi.org/10.1080/02786820490251358

Von Der Weiden, S.L., Drewnick, F., Borrmann, S., 2009. Particle loss calculator - A new software tool for the assessment of the performance of aerosol inlet systems. Atmos. Meas. Tech. 2, 479–494. https://doi.org/10.5194/amt-2-479-2009

William C. Hinds, 1999. Aerosol Technology Properties Behavior and Measurement of Airborne Particles, 2nd ed, A Willey-Interscience Publication John Willey & Sons, Inc. https://doi.org/10.1533/9781845695750.frontmatter